Expanded View Figures

Figure EV1. GSL synthesis inhibition does not inhibit neural differentiation.

A Schematic representation of Myriocin, Fumonisin B1, NB-DNJ, PPMP, and GM3S silencing (siGM3S) mediated inhibition of GSL synthesis.

B Effect of NB-DNJ (25 μM) and PPMP (2.5 μM) treatment on sphingolipid synthesis in E14-mESCs. E14-mESC control, treated with NB-DNJ or PPMP, was pulse-labelled as for 8 h with [^{3}H]-sphingosine. Sphingomyelin (SM) and GSL synthesis in control (grey), NB-DNJ (cyan)-, and PPMP (orange)-treated cells are expressed as percentage of control ± SD from three independent experiments. $^{**}P \leq 0.01$.

C E14-mESCs induced to differentiate into neurons over 13 days in the presence of NB-DNJ (25 μM) or PPMP (2.5 μM) were analysed by cytofluorometry with antibodies directed against the ganglioside GT1b. Cytofluorimetric profiles are shown for cells treated with NB-DNJ (cyan), or PPMP (orange) or with vehicle (grey). Arrows indicate the direction of changes induced by each treatment.

D E14-mESCs were kept in an undifferentiated state (day 0) or induced to differentiate into neurons over 13 days in the presence of NB-DNJ (25 μM), PPMP (2.5 μM), or vehicle (methanol). Subsequently, cells were lysed and lysates were processed for SDS–PAGE and immunoblotting using antibodies against the stemness markers Oct-4, and Nanog and the neuronal marker Tuj-1.

E E14-mESCs induced to differentiate into neurons in the presence of Myriocin (2.5 μM) or Fumonisin B1 (FB1) (25 μM) were analysed as in (C). Cytofluorimetric profiles are shown for cells treated with Myriocin (red), or FB1 (purple) or with vehicle (grey). Arrows indicate the direction of changes induced by treatments.

F E14-mESCs in an undifferentiated state (day 0) or induced to differentiate into neurons in presence of Myriocin (2.5 μM), Fumonisin B1 (FB1) (25 μM), or vehicle (methanol). Subsequently, cells were lysed and lysates were processed as in (D).

G E14-mESCs induced to differentiate into neurons and subjected every 3 days to GM3S silencing by transfecting specific siRNA for murine GM3S mRNA (siGM3S) were analysed by cytofluorometry as in (C). Cytofluorimetric profiles are shown for cells treated with non-targeting siRNA (grey), or with specific siGM3S (green). Arrows indicate the direction of changes induced by treatments.

H E14-mESCs were induced to differentiate into neurons and transfected every 3 days with siGM3S were subjected to RNA extraction and RT–PCR to evaluate the efficiency of murine GM3S silencing. Data are means ± SD from two independent experiments.

I E14-mESCs treated as in (G) were lysed, and lysates were processed for SDS–PAGE and immunoblotting as in (D).

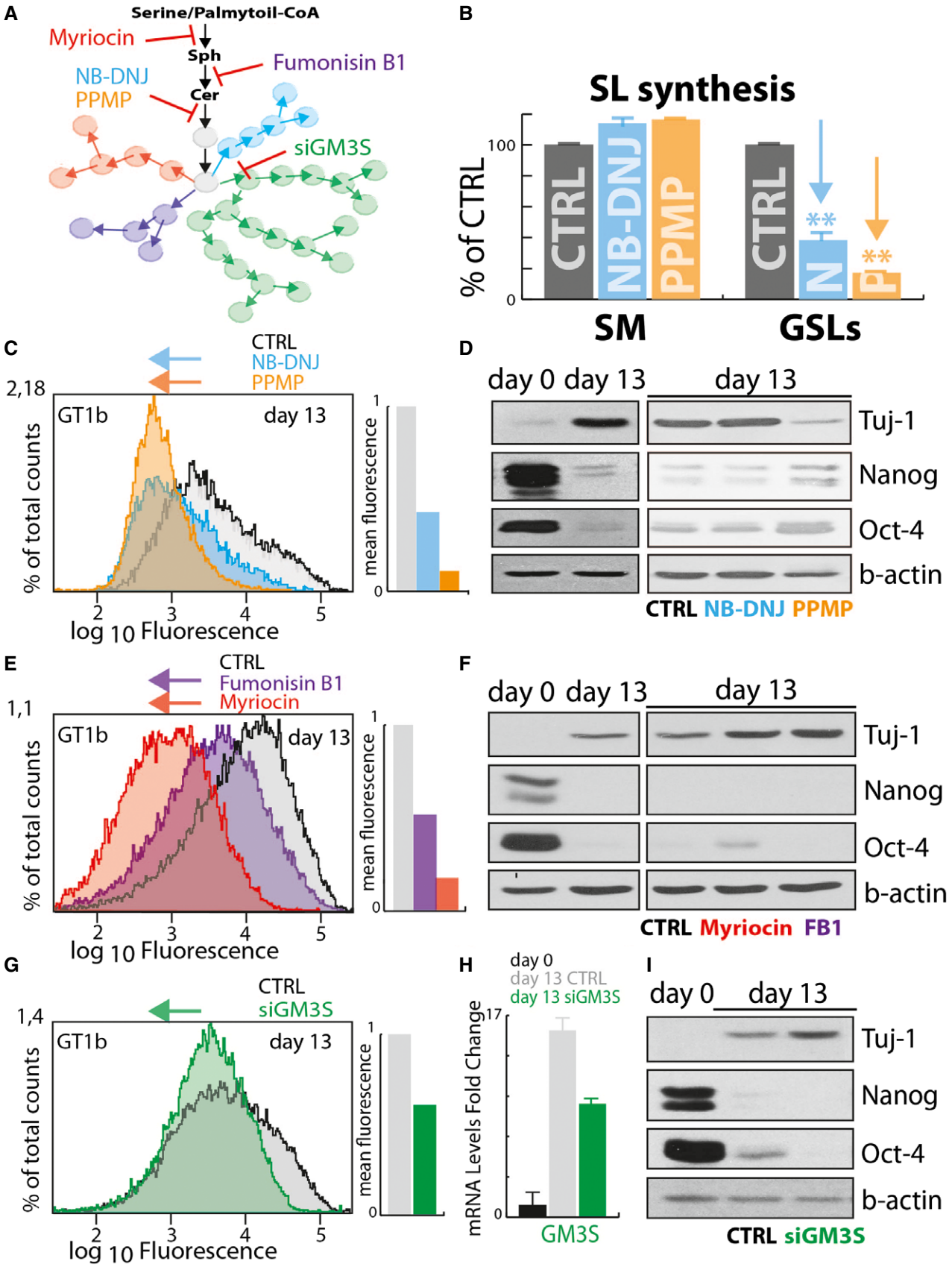

Figure EV1.

Figure EV2. GSL production in non-neural cells recapitulates the GSL switch at the single-cell level.

A ChTxB and ShTxB double-positive cells were isolated by FACS and seeded, and either imaged immediately (left panel) or after 5 days of growth (right panel) as in Fig 3A. Scale bar, 50 μm.

B HeLa cells plated on gridded glass-bottomed tissue culture dishes and imaged by phase contrast microscopy over 72 h (see also Movie EV1). After fixing, the cells were stained with Alexa488-ChTxB (green), Cy3-ShTxB (red), and DAPI (blue). Confocal images were acquired of the same fields imaged by video microscopy. Scale bar, 50 μm. Twenty-four cells were followed for two cell divisions, to yield 96 daughter cells, where the ShTxB positivity and ChTxB positivity were assessed by confocal microscopy. The dendrogram (bottom right) shows how 10/24 cells gave only ShTxB-positive offspring, 2/24 gave only ChTxB-positive offspring, 10/24 gave double-negative offspring, and only two parental cells gave mixed offspring. The probability of 10/24 parental cells to randomly yield a ShTxB-only positive offspring and the probability of 2/24 parental cells to randomly yield a ChTxB-only positive offspring are indicated in the dendrogram and are calculated as detailed in Appendix Methods.

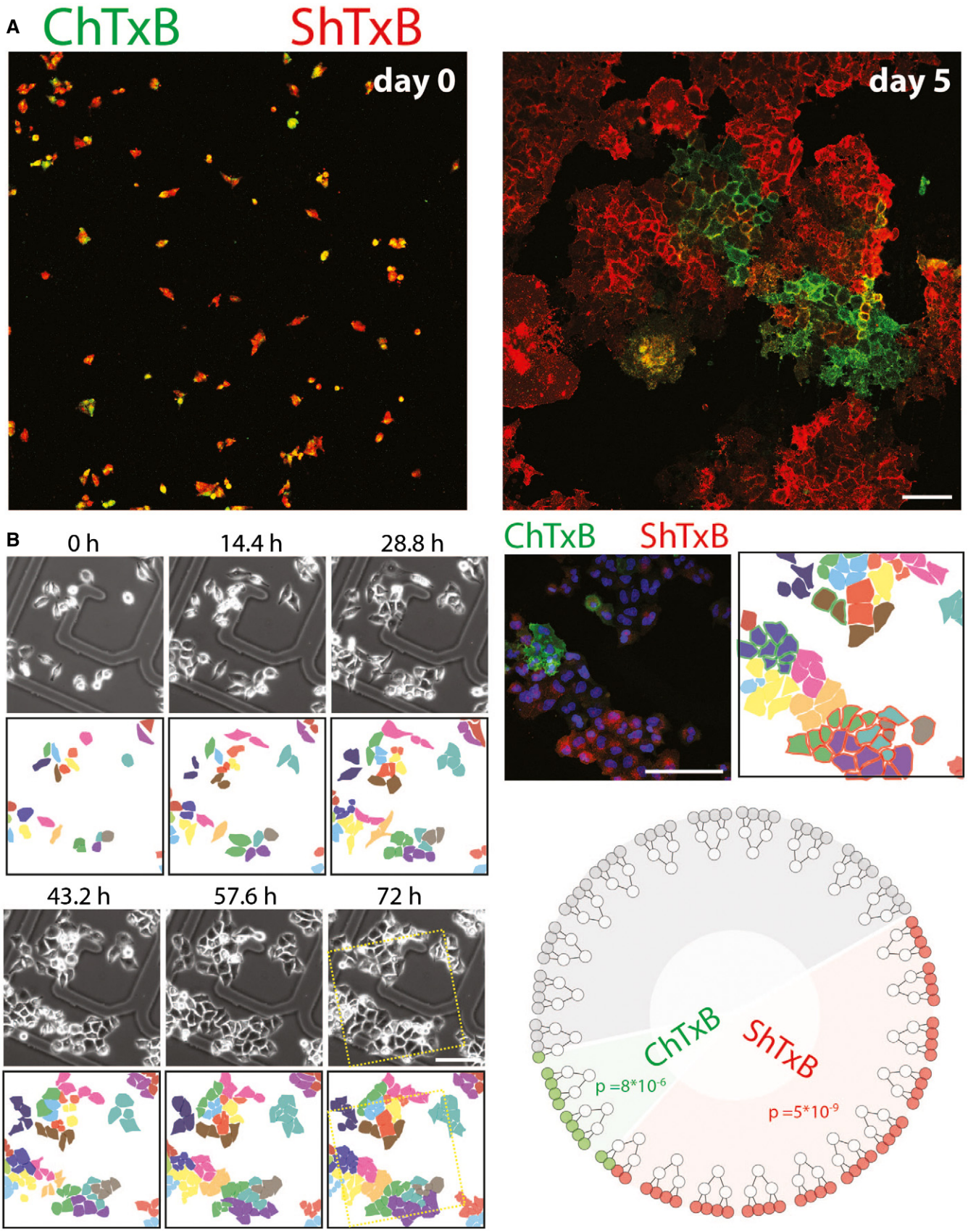
A
ChTxB
ShTxB
day 0
day 5
B
0 h
14.4 h
28.8 h
43.2 h
57.6 h
72 h
ChTxB
ShTxB
ChTxB
ShTxB
p =8*10-6
p =5*10-9

Figure EV2.

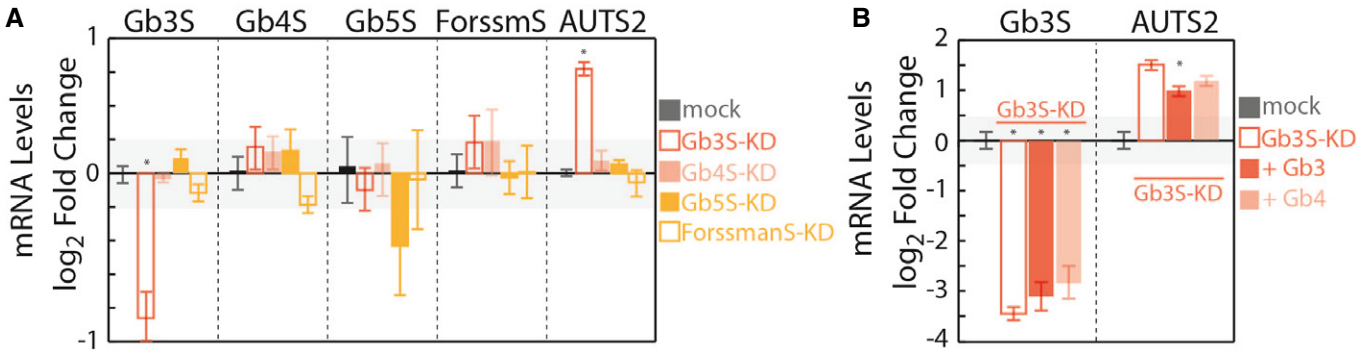

Figure EV3. Globo-series GSLs regulate AUTS2 expression.

A Effects of silencing globoside-synthesising enzymes Gb3S, Gb4 synthase (Gb4S), Gb5 synthase (Gb5S), and Forssman antigen synthase (ForssmanS or ForssmS) on mRNA levels of AUTS2. Silenced cells were subjected to RNA extraction and RT–PCR to evaluate both the efficiency of silencing and AUTS2 mRNA up-regulation (measured as detailed in the Appendix and expressed as $\log_2$-fold changes to mock-treated cells). Data are means ± SD from at least three independent experiments. *$P \leq 0.05$ compared to mock treated cells.

B Effect of exogenous Gb3 and Gb4 on AUTS2 expression in Gb3S-KD cells. HeLa cells were either mock-treated or silenced for Gb3S expression. Gb3S-KD cells were then either vehicle-treated or fed with the indicated GSLs (10 μM). Gb3S and AUTS2 mRNA levels (as $\log_2$-fold changes to mock) under the different treatments are reported. Data are means ± SD from at least three independent experiments. *$P \leq 0.05$ compared to Gb3S-KD.

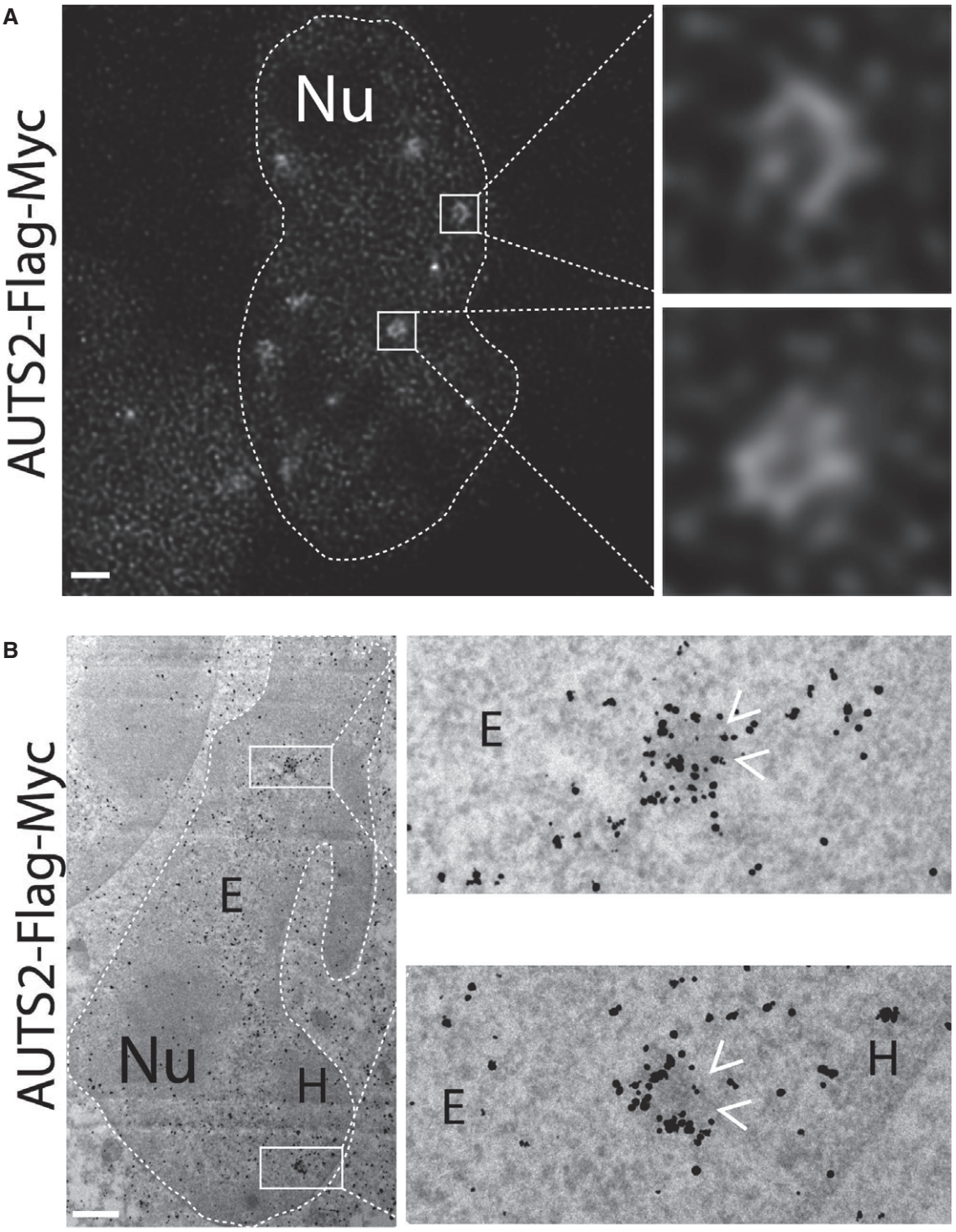

Figure EV4. AUTS2 surrounds heterochromatic bodies in the nucleus.

A AUTS2 localisation evaluated by gated-STED nanoscopy using anti-Flag antibody.

B HeLa cells expressing human AUTS2-Flag-Myc were processed for immuno-electron microscopy as detailed in the Appendix. Antibody directed against Flag tag was used to detect the expressed protein. Arrowheads indicate the heterochromatic granules decorated by AUTS2.

Data information: Nu, nucleolus; H, heterochromatin; E, euchromatin. Scale bars, 1 μm.

Figure EV5. The Gb3–AUTS2 axis controls histone acetylation at neural genes promoters.

A Scatter plot of normalised ChIP-seq values associated with 15,040 common H3K9/14Ac peaks in mock-treated HeLa cells compared to Gb3S-KD cells (red) or AUTS2-KD cells (cyan) (see Dataset EV2 for peak positions and values data; this dataset has been registered to GEO database with the following accession number GSE107044).

B Scatter plot of Gb3S-KD/mock versus AUTS2-KD/mock normalised $\log_2$ ChIP-seq value ratios for 1,896 common H3K9/14Ac peaks bound by AUTS2 (blue) and 13,144 non-AUTS2-bound peaks (orange).

C % frequency distribution of Gb3S-KD/mock (red) and AUTS2-KD/mock (cyan) $\log_2$ ChIP-seq value ratios for AUTS2-bound and non-AUTS2-bound H3K9/14Ac peaks.

D Representative H3K9/14Ac ChIP-seq profiles for AUTS2-bound promoters. Blue rectangles indicate AUTS2 binding sites; black arrows indicate transcriptional start sites.

E Tissue distribution of genes intercepted by the 1,809 H3K9/14Ac peaks occupied by AUTS2 (source, David Ontology).

F HeLa cells silenced for AUTS2 in control cells and in cells silenced for Gb3S. qPCR was performed to determine knock-down efficiencies and the mRNA changes in selected genes intercepted by the H3K9/14Ac peaks occupied by AUTS2. mRNA levels are expressed as $\log_2$-fold changes with respect to mock-treated cells. Data are means ± SEM of at least three independent experiments. $^{*}P \leq 0.05$ to mock; $^{\S}P \leq 0.05$ to AUTS2-KD.

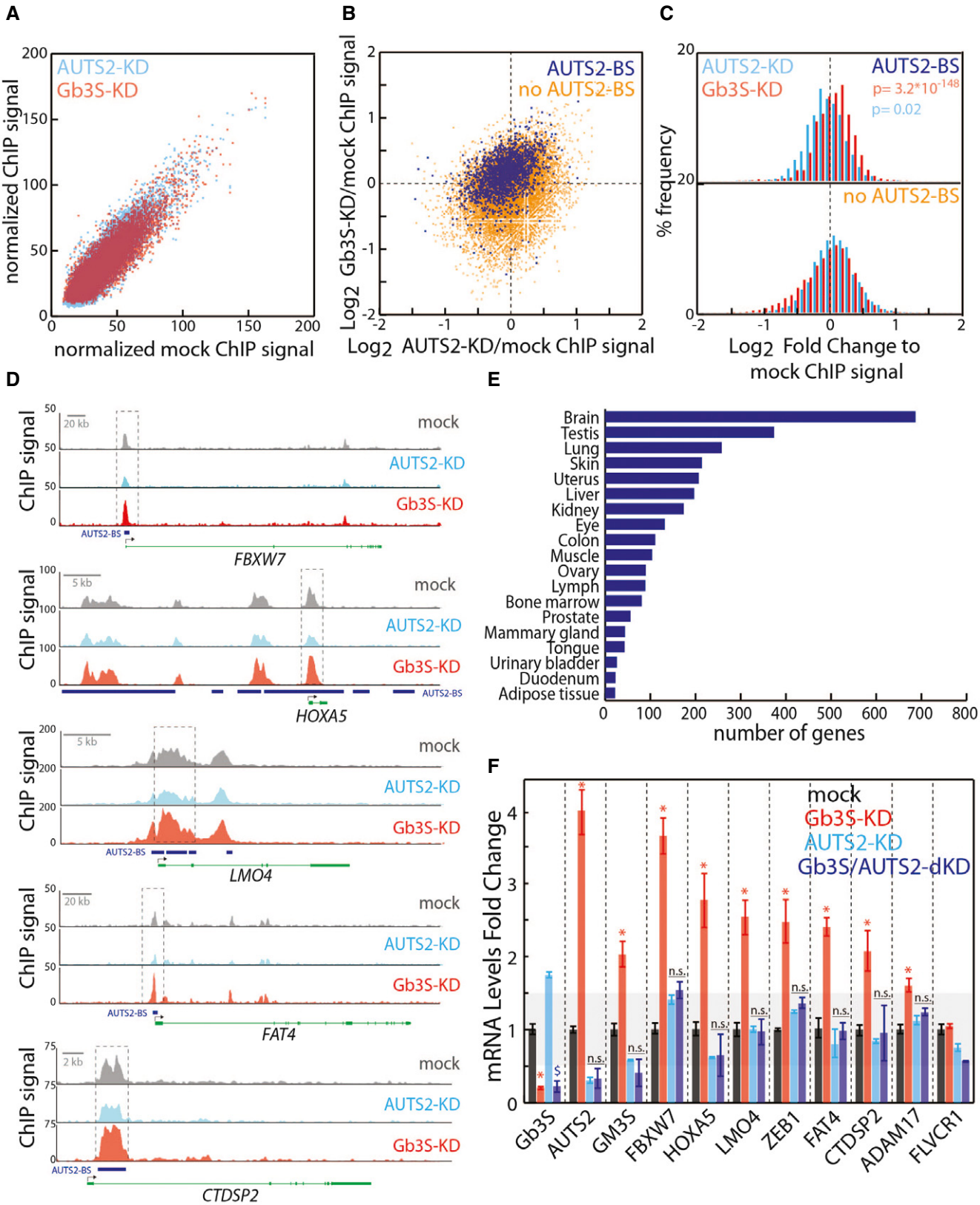

Figure EV5.

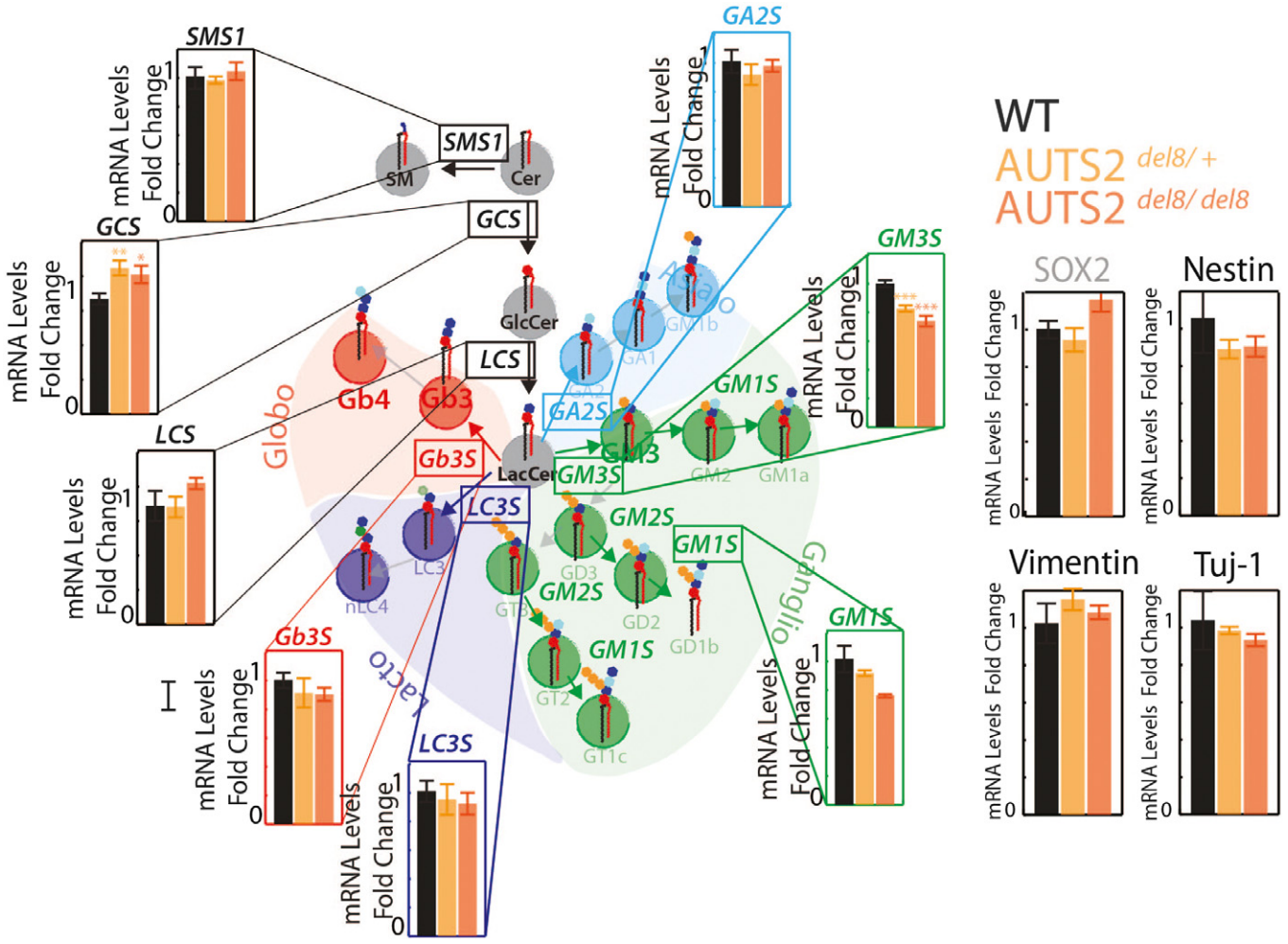

Figure EV6. AUTS2 controls GM3S expression in mouse brain.

Whole brains from wild-type (n = 5), AUTS2 heterozygous KO (AUTS2$^{del8/+}$; n = 5), and AUTS2-KO (AUTS2$^{del8/bel8}$; n = 5) mouse embryos (E 17.5) were processed for mRNA extraction. qPCR was used to determine the mRNA levels of the indicated genes. Data are means ± SEM.